Journal of Science: Advanced Materials and Devices 1 (2016) 105–112

Contents lists available at ScienceDirect

Journal of Science: Advanced Materials and Devices

journal homepage: www.elsevier.com/locate/jsamd

Review article

d-magnetism instability in *R*-Co intermetallic compounds

Irina Yu. Gaidukova [a], Ashot S. Markosyan [b, *]

[a] Faculty of Physics, M.V. Lomonosov Moscow State University, 119991 Moscow, Russia
[b] Edward L. Ginzton Laboratory, Stanford University, California 94305, USA

ARTICLE INFO

Article history:
Received 13 June 2016
Accepted 13 June 2016
Available online 18 June 2016

Keywords:
Magnetic phase transitions
Magnetic structures
Itinerant magnetism
Ferrimagnetism
Rare earth intermetallics

ABSTRACT

Magnetic phenomena observed in *R*-Co intermetallic compounds with the *d*-magnetism instability are reviewed. The magnetic instability in these compounds is intimately related to the special position of the Fermi level in the hybridized 3*d*-5*d* (4*d*) band near to a local peak in $N(\varepsilon)$. In the presence of the *f*-*d* exchange interaction the magnetic state of the itinerant electron subsystem can essentially be modified giving rise to a number of field- and temperature-induced magnetic phase transitions. Following the band structure calculations these transitions as well as most of their fine details can be well understood theoretically. Magnetic, magnetoelastic and transport measurements of some *R*-Co compounds with *d*-magnetism instability and pseudobinary systems with *R* and Co substituted by either magnetic or nonmagnetic elements are presented and discussed.

1. Introduction

In rare earth (RE) – cobalt, *R*-Co, intermetallic compounds the Co itinerant magnetic sublattice shows a variable magnetic moment. It shows a paramagnetic behaviour in compounds of the RE-rich side (R_3Co), is ferromagnetic with a stable magnetic moment of 1.6 μ_B/Co in the Co-rich side (R_2Co_{17}) (Fig. 1) [1–3]. In the middle of this series the Co magnetic moment substantially depends on the RE sublattice, i.e. the type of the RE ion. In RCo_2 intermetallics the Co sublattice changes from a paramagnetic to a ferromagnetic state depending on the strength of the *f*-*d* exchange interaction (molecular magnetic field) and changes from a weak to strong magnetic state in RCo_3 and R_4Co_3 compounds (see, e.g. Ref. [3]).

The magnetic properties of *R*-Co intermetallic compounds with instable Co magnetic sublattice show in general more diverse and richer behaviour compared to the compounds with stable itinerant-electron magnetic sublattice. In this article some of the most characteristic effects the *R*-Co intermetallics exhibit due to the Co magnetism instability are reviewed. Much work in this field, especially in studying field-induced magnetic phase transitions in RCo_2 and RCo_3 intermetallic compounds was done by Peter Brommer with the colleagues [4–9].

Nature of magnetism is different in two electron subsystems involved in the magnetic interactions in the *R*-Co intermetallics. Most of the lanthanide ions retain the localized atomic character of the 4*f* orbitals and their magnetism can be well described by atomic characteristics, *L*, *S* and *J*, of a free R^{3+} ion. In contrast, the 3*d*-electrons of cobalt sublattice are itinerant and the 3*d*-states form an energy band crossed by the Fermi level ε_f with natural consequences for magnetism (see, e.g., Ref. [1,3]). The interaction between the RE and Co sublattices occurs mostly through hybridization of the 5*d* (4*d*)-states of RE and the 3*d*-states of the transition metal, which mediates the strength of the 4*f*-3*d* exchange interaction.

The effect of the RE sublattice on the magnetic properties of the *d*-subsystem is in most cases considered as resulting in an additional shift of the majority and minority *d*-subbands, whereas the effect of the *d* electrons on the RE sublattice consists in the modification of the energy level scheme of the R^{3+} ions.

Because of a spatial localization of the 4*f* electronic shells, no direct overlap between the 4*f* wave functions takes place in the *R*-3*d* intermetallics and the *f*–*f* exchange occurs via the conduction electrons. The interactions related to the *d*-sublattice increase successively along with the content of the transition metal and the *d*–*d* interaction becomes dominating in the Co-rich compounds.

2. Itinerant magnetism of the d-electron subsystem and density of states - theoretical background

The main distinct feature of *d*-magnetism in *R*-3*d* intermetallics, which makes the magnetic properties of the Co sublattice

* Corresponding author.
E-mail address: ashotm@stanford.edu (A.S. Markosyan).
Peer review under responsibility of Vietnam National University, Hanoi.

http://dx.doi.org/10.1016/j.jsamd.2016.06.008

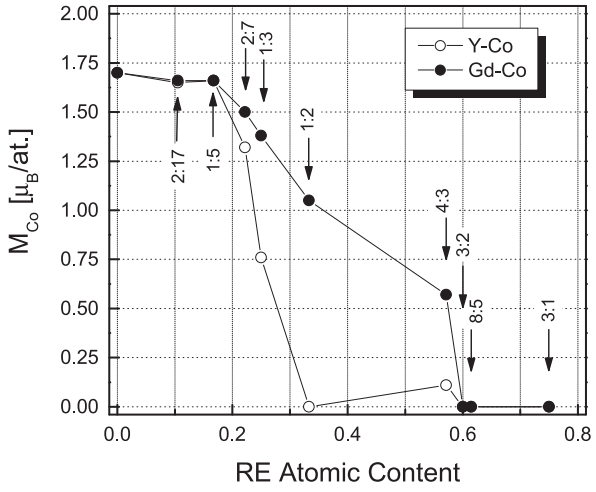

Fig. 1. Co-magnetic moment versus Y and Gd content in Y-Co and Gd-Co intermetallic compounds [2].

dependent on stoichiometry, is the hybridization between the narrow 3*d* band (~3 eV) of the transition metal with a high density of states (DOS), $N_{3d}(\varepsilon)$, and the broader 5*d* band (~10 eV) of lanthanide (the 4*d* band of Y) with lower DOS. The contribution to the total DOS from the 6*s* (5*s*) band is negligible because of low $N_s(\varepsilon)$. The magnetic properties of the *d*-electron subsystem are hence determined by the energy dependence of $N_d(\varepsilon)$ near the Fermi level, ε_f, and the position of ε_f itself [2,3,8].

The most known *R*-Co intermetallics with the *d*-magnetism instability are the RCo_2 compounds, in which the *d*-electron subsystem exhibits itinerant electron metamagnetism (IEM), i.e., a first-order field-induced magnetic phase transition from a paramagnetic to ferromagnetic state [10–12]. For the YT_2 compounds with T = Fe, Co and Ni several authors have published band structure calculations. Although for these calculations different methods have been used (e.g. Ref. [13,14]), the common result of all these calculations confirms the existence of a strong hybridization between the 3*d* states of the transition metal and 4*d* states of yttrium (or 5*d* states in the case of a lanthanide). The calculated energy dependence of DOS is qualitatively similar in shape for all these intermetallics. At low energies $N(\varepsilon)$ exhibits a relatively narrow peak (due to the 3*d* electronic states) followed by a flat range with lower DOS at greater energies (primarily due to the 4*d* states).

In Fig. 2, $N(\varepsilon)$ near ε_f of YFe_2, YCo_2 and YNi_2 are compared [13]. Among them YNi_2 has the lowest value of $N(\varepsilon_f)$. The Stoner criterion of ferromagnetism $IN(\varepsilon_f) \geq 1$ (I is the d–d exchange integral) is by far not fulfilled, the product $IN(\varepsilon_f) = 0.21$. YNi_2 is nonmagnetic and shows a very weak temperature dependence of susceptibility. In contrast, $IN(\varepsilon_f) = 2.6$ for YFe_2, which is therefore is a ferromagnet with a spontaneous magnetization $M_S = 1.4$ μ_B/Fe at 4.2 K. Since M_S of YFe_2 is considerably smaller than M_S for metallic Fe (=2.2 μ_B/Fe), YFe_2 is a non-saturated ferromagnet, i.e. the spin-up and spin-down bands both are not filled. For YCo_2 the Stoner criterion is nearly fulfilled: $IN(\varepsilon_f) = 0.9$. This causes a strong exchange enhancement with a pronounced temperature variation of the magnetic susceptibility. The average value of χ is much larger than the Pauli susceptibility.

For YT_3 compounds, the calculated energy dependence of DOS is shown in Fig. 3 [14]. The shapes of DOS of YFe_3, YCo_3 and YNi_3 are again more or less similar to each other as in the case of YT_2 compounds. While ε_f of YFe_3 is located near the highest peak of the DOS that of YCo_3 is located near a steep descent of the $N(\varepsilon)$ and that of YNi_3 is located just above a small peak. As a result, YCo_3 is a weak

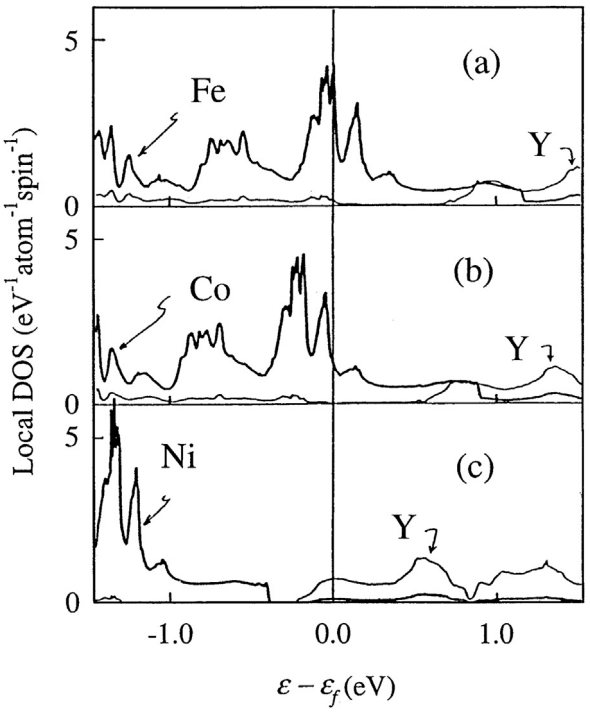

Fig. 2. Calculated local DOS of the 3*d* electrons of *T* and 4*d* electrons of Y for YFe_2 (a), YCo_2 (b), and YNi_2 (c) in the paramagnetic state [13].

itinerant electron ferromagnet with T_C varying from 280 to 301 K and M_S from 1.35 to 1.45 μ_B/f.u.

The calculated electronic structure of Y_4Co_3 is shown in Fig. 4 [15]. This compound has a Ho_4Co_3-type hexagonal crystal structure with three inequivalent Co sites (6*h*), (2*d*), (2*b*) and two inequivalent Y sites. As the unit cell includes three formula units, the Co(2*b*) sites are half-filled (50%) and the number of atoms in the unit cell is equal to 21. Thus, in this crystallographic model, Y_4Co_3 cannot be regarded as an ordered compound, but as a disordered alloy with (2*b*) sites occupied randomly by cobalt atoms and vacancies. The ferromagnetic state obtained from spin-polarized computations is attributed to the Co atoms located on the (2*b*) sites, being the only magnetic atoms among 21 ones in the unit cell, and forming a quasi-one dimensional magnetic chains. As seen, in this case the Fermi level is located on an expressed minimum of DOS. Thus application of either external or internal molecular magnetic field shall result in an increase of the total DOS and a stronger polarization of the *d*-band with corresponding increase of the magnetic moment per Co.

In the above *R*-Co series, substitutions of non-magnetic Y by magnetic RE induces a substantial increase of μ_{Co}. Within the scope of the itinerant model, this effect is ascribed to the *f*-*d* exchange interaction. The total molecular field acting on the *d* subsystem reads [1,3].

$$B_{mol}^{(Co)} = \lambda_{dd} M_d + \lambda_{Rd} M_R, \quad (1)$$

where $\lambda_{dd} = z_d I_{dd}/2\mu_B^2$ and $\lambda_{dd} = (g_R - 1) z_R I_{Rd}/2 g_R \mu_B^2$ are the corresponding molecular field coefficients, I_{dd} and I_{Rd} denote the d–d and *R*-*d* exchange integrals, z_d and z_R are the numbers of *T* and *R* atoms in the nearest-neighbour surrounding to a *T* atom. In the presence of external magnetic field, the total effective field acting on the Co sublattice can be represented as

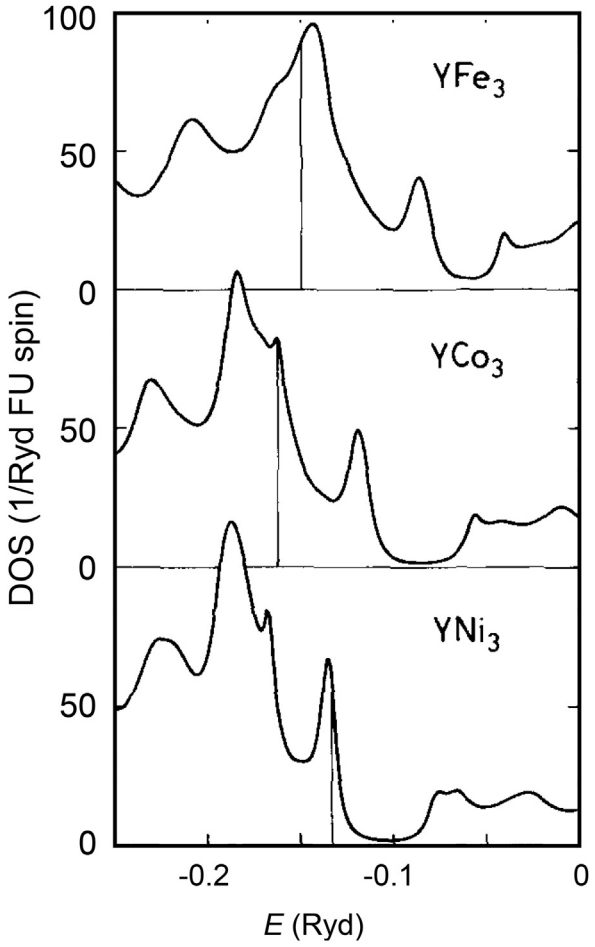

Fig. 3. The DOS calculated for YFe_3, YCo_3 and YNi_3. Vertical lines show the position of the Fermi levels [14].

$$\boldsymbol{B}_{eff}^{(Co)} = \boldsymbol{B}_{mol}^{(Co)} + \boldsymbol{B}_{ext} = \boldsymbol{B}_{RCo}^{(Co)} + \boldsymbol{B}_{CoCo} + \boldsymbol{B}_{ext} = \lambda_{RCo}\boldsymbol{M}_R + \lambda_{CoCo}\boldsymbol{M}_{Co} + \boldsymbol{B}_{ext}, \quad (2)$$

where $\boldsymbol{B}_{RCo}^{(Co)}$ and $\boldsymbol{B}_{CoCo}$ arise from the intersublattice and intra-sublattice exchange interactions, respectively, and λ_{RCo} and λ_{CoCo} are the corresponding molecular field coefficients.

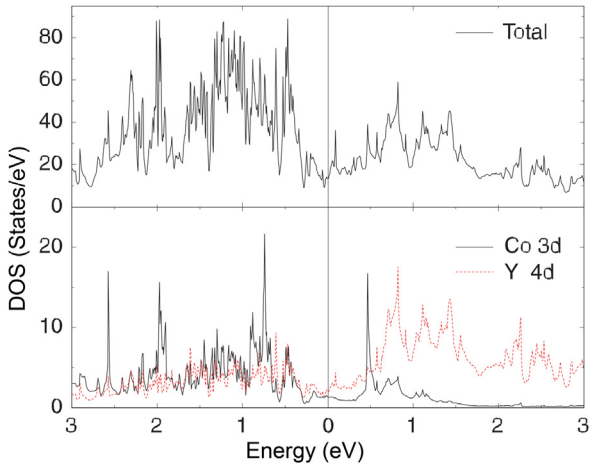

Fig. 4. The total and atom-projected density of states of Y_4Co_3. The contribution of Co 3*d* and Y 4*d* to density of states [15].

Since in the above *R*-Co intermetallics $B_{RCo}^{(Co)}$ is much larger than B_{CoCo}, the molecular field acting on the Co sublattice can be set proportional to the magnetization of the *R* sublattice M_R. Assuming that the dependence of I_{RCo} on the *R* element is weak, the magnetic field acting on the Co sublattice is then proportional to $(g_R - 1)S_R$. This approximation can frequently be applied for qualitative understanding of the magnetization process in some *R*-Co intermetallics although with stronger Co magnetic state λ_{CoCo} must certainly be taken into account [3].

3. IEM in RCo_2 intermetallics

3.1. RCo_2 compounds with non-magnetic R

The RCo_2 intermetallics are primarily known for the metamagnetic transition the *d*-electron subsystem undergoes in strong magnetic fields at some critical value B_M. Also in the case of a ferromagnetic ground state, if there is a field induced increase of $N(\varepsilon_f)$, IEM can occur from a weak ferromagnetic to a strong ferromagnetic state [16].

Goto et al. first experimentally observed IEM in YCo_2 (70 T) and $LuCo_2$ (75 T) [17]. A number of studies have been performed in order to understand why substitutions of Co by non-magnetic ions lower B_M. Three mechanisms were discussed: *i*) a shift of ε_f due to the change of the *d* electron concentration [18], *ii*) a change of the d-bandwidth due to the variation of the lattice parameter [19], and *iii*) in the case of a non-transition metal substitution, the hybridisation between the *d* states and 3*p* states of *T* has been made responsible.

In Ref. [20] the variation of B_M vs. *x* was compared in $Y(Co_{1-x}Al_x)_2$, $Lu(Co_{1-x}Al_x)_2$, and $(Y_{1-t}Lu_t)(Co_{1-x}Al_x)_2$ system. The third one has been selected to keep the lattice parameter constant due to the simultaneous Al and Lu substitutions. It has been concluded that the change in the interatomic distances has less influence than the change of the *d*-electron concentration. In Ref. [21] the $Y(Co_{1-x}Ni_{0.5x}Fe_{0.5x})_2$ system has been investigated with $x \leq 0.03$. It has been reported that B_M does not change significantly when the *d*-electron concentration is constant.

The interpretation of all the above results was made under the rigid band approximation. However for higher amount of substitution this approximation is no longer valid. In Ref. [22] it was pointed out that the hybridization between the 3*d*-states of Co and 3*p* states of the substituent non-transition *T* atoms becomes important for higher *x*. The calculations of DOS for $Y(Co_{0.75}Al_{0.25})_2$ revealed that this hybridization causes a substantial change of the shape of $N(\varepsilon)$ around ε_f. The peak in DOS below $N(\varepsilon_f)$, which is responsible for IEM and for the appearance of ferromagnetism in the $R(Co_{1-x}Al_x)_2$ systems, is smeared out.

3.2. Effect of the f-d intersublattice exchange

The metamagnetic behaviour of the Co-sublattice within the RCo_2 compounds can clearly be seen when plotting M_{Co} vs. $B_{mol}^{(Co)}$ (Fig. 5) [23]. The symbols on this plot depict the M_{Co} values as obtained from thermal expansion and magnetization measurements. This figure shows that for all the RCo_2 compounds (except $TmCo_2$) $B_{RCo}^{(Co)} > B_M$ thus stabilizing a ferromagnetic order in the Co sublattice. In $TmCo_2$ the Co sublattice remains non-magnetic below T_C [24]. Brommer et al. [25] determined $B_{mol}^{(Co)} = 54$ T for $TmCo_2$, which is below the value of $B_M = 70$ T necessary to induce ferromagnetic order in the Co sublattice. The magnetization curve of YCo_2 [17] included in Fig. 5 for comparison fits well the general tendency of M_{Co} vs. $B_{mol}^{(Co)}$.

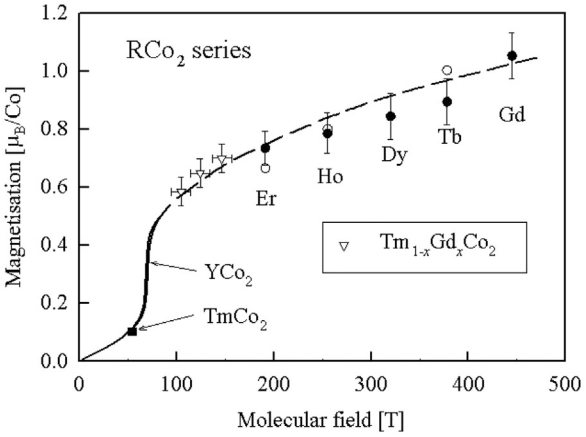

Fig. 5. Variation of the *d*-magnetic moment μ_{Co} versus B_{RCo} derived from X-ray powder diffraction data of RCo_2 (full circles) and $Tm_{1-x}Gd_xCo_2$ (open down triangles). Open circles represent the single-crystal magnetization data taken from literature [3]. μ_{Co} for $TmCo_2$ is taken from the neutron diffraction data [45]. The solid line is the experimental magnetization curve of YCo_2 [17], the dashed line is drawn as a guide for the eyes.

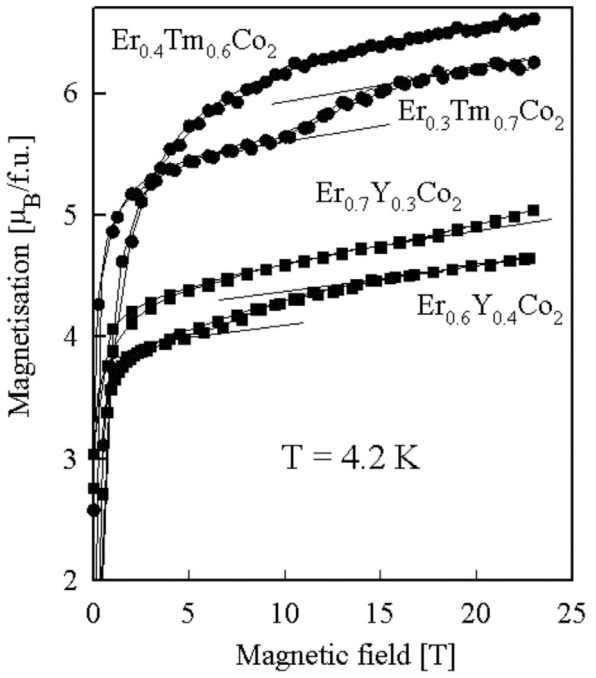

Fig. 6. Magnetization curves at 4.2 K of some selected $Er_{1-x}R_xCo_2$ (R = Y or Lu) compounds [28]. The solid straight lines are linear extrapolations from the field regions below and above B_{cr}. $Er_{0.3}Tm_{0.7}Co_2$ and $Er_{0.6}Y_{0.4}Co_2$ show inverse IEM at 12 T and 8.5 T, respectively. For $Er_{0.7}Y_{0.3}Co_2$ the critical field exceeds 25 T, however above 20 T an upturn can be seen in the magnetization curve.

In all RCo_2 compounds M_R is greater than M_{Co}. The external field is therefore parallel to M_R, thus the effective field acting on the Co sublattice decreases (for heavy RCo_2) with increasing external field: $\boldsymbol{B}_{eff}^{(Co)} = \boldsymbol{B}_{mol}^{(Co)} - \boldsymbol{B}_{ext}$. If B_{ext} exceeds a critical field B_{cr}, the Co sublattice magnetization is destabilised and so-called 'inverse IEM' may occur. This inverse IEM is visible, e.g., as a step-like increase in the magnetization process. Above B_{cr} long range magnetic order exists in the R sublattice only. This field can be reduced by substitutions. For $R_{1-x}Y_xCo_2$ systems the concentration dependence of B_{cr} is given by:

$$\boldsymbol{B}_{cr}(x) \approx (1-x)\lambda_{RCo}\boldsymbol{M}_R - \boldsymbol{B}_M \tag{3}$$

Among the heavy RCo_2 compounds, $ErCo_2$ has the lowest value of $B_{mol}^{(Co)} = 190$ T (see Fig. 5) and therefore the lowest expected value of B_{cr}. Transitions of this type have been observed in the $Er_{1-x}Y_xCo_2$ and $Er_{1-x}Lu_xCo_2$ systems on the $M(B)$ magnetic isotherms, magnetostriction, and magnetoresistance [26–28]. Magnetic isotherms showing the inverse IEM effect are displayed in Fig. 6. The transition occurs in $Er_{0.3}Tm_{0.7}Co_2$ (12 T) and $Er_{0.6}Y_{0.4}Co_2$ (8.5 T) in agreement Eq. (3).

Another interesting effect observed in RCo_2 compounds is that with R = Dy, Ho and Er the magnetic phase transition at T_C is of a first-order type. This is again related with the metamagnetic properties of the *d* electron subsystem (see, e.g., Ref. [11,29]). The conditions for the occurrence of a first-order transition at T_C have been given in Ref. [30] within the scope of the molecular field approximation and assuming that the *d* subsystem is identical throughout the whole RCo_2 series. It was concluded that this transition is of a first-order type when $T_C < 150$ K.

In Ref. [31] was shown that a ferrimagnetic system like RCo_2, can be decoupled if one of the sublattices exhibits a magnetic instability. This phenomenon takes place when (setting $B_{RR}^{(Co)}$ zero)

$$B_{RCo}^{(Co)} < B_{cr} \tag{4a}$$

at $T = T_C^{(R)}$ of the R sublattice, and

$$B_{RCo}^{(Co)} > B_{cr} \tag{4b}$$

holds at 0 K. For these selected compounds the critical condition for the onset of magnetic order in the Co sublattice is not fulfilled at $T_C^{(R)}$; however it will be fulfilled on further cooling thus resulting in a second transition at $T = T_C^{(Co)} < T_C^{(R)}$. A separate ordering of two magnetic sublattices can be anticipated in substituted $R'_{1-x}R''_xCo_2$ compounds within a limited concentration range [26].

As an example, Fig. 7 displays two separated ordering temperatures ($T_C^{(R)}$ and $T_C^{(Co)}$) observed experimentally in the $Er_{1-x}Y_xCo_2$ system [31]. In the Er-rich region only one anomaly can be seen, which corresponds to the onset of long-range magnetic order in both sublattices. For $Er_{0.6}Y_{0.4}Co_2$, two maximums are observed in the specific heat. From the volume effect accompanying the lower transition it follows that $T_C^{(Co)} = 11$ K, while the R sublattice orders at higher temperature $T_C^{(R)} = 14.5$ K.

3.3. Field induced non-collinear magnetic structures in presence of a magnetic instability

In ferrimagnets between certain critical fields B_{m1} and B_{m2} non-collinear magnetic structures are stable with a linear dependence of M_{tot} vs. B_{ext}. At $B_{ext} > B_{m2}$ the structure is ferromagnetic [32].

In ferrimagnets with an unstable magnetic sublattice, like RCo_2 compounds, the magnetization processes can substantially be modified. If the magnetization of the unstable sublattice (M_{Co}) is less than that of the stable one (M_R) and B_M is less than the lower critical field B_{c1}, non-collinear magnetic structures will not appear. The system will become ferromagnetic through two IEM transitions: *i*) a disappearance of the Co magnetic moment at a critical field B_{m1} and *ii*) a re-entrant onset of the Co magnetic moment along the field direction at a field $B_{m2} > B_{m1}$ [33]:

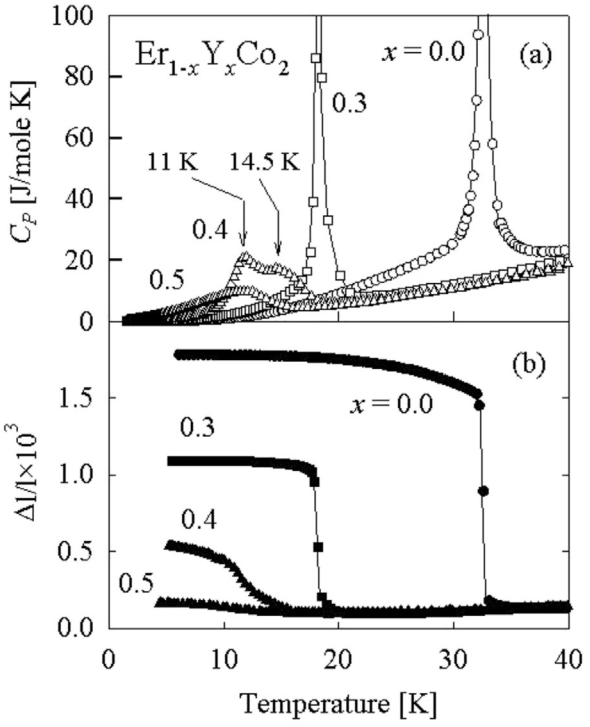

Fig. 7. The temperature-dependent specific heat C_P (a) and linear thermal expansion (b) of the $Er_{1-x}Y_xCo_2$ compounds with $x = 0$, 0.3, 0.4 and 0.5 [31]. Arrows indicate the two transitions resolved in $Er_{0.6}Y_{0.4}Co_2$.

$$\begin{cases} M_{tot} = M_R - M_{Co}, & B_{ext} < B_{m1} = \lambda_{RCo} M_R - B_M \\ M_{tot} = M_R, & B_{m1} < B_{ext} < B_{m2} = \lambda_{RCo} M_R + B_M \\ M_{tot} = M_R + M_{Co}, & B_{ext} > B_{m2} \end{cases} \quad (5)$$

Depending on the intrinsic parameters, different magnetization processes and even overlapping of IEM and a transition into a non-collinear phase can occur. For experimental observation, internal parameters B_M, λ_{RCo}, M_R or M_{Co} can be changed using appropriate R and Co substitutions. The comparison between B_M and B_{m1} shows that in all the ferrimagnetic RCo_2 compounds the magnetization process must follow the expressions given by equation (5).

In Ref. [34] the $(R_{1-t}Y_t)(Co_{1-x}Al_x)_2$ systems were studied, in which the Co sublattice shows magnetic instability. For $(Ho_{0.8}Y_{0.2})(Co_{0.925}Al_{0.075})_2$ the conditions given by equation (5) are fulfilled and no non-collinear structures were observed in the magnetization process. Instead, metamagnetic transitions occur at 13 and 72 T.

Brommer et al. [25] studied the $(Tm_{1-t}Lu_t)(Co_{0.88}Al_{0.12})_2$ system with a stable Co sublattice in fields up to 28 T. $Lu(Co_{0.88}Al_{0.12})_2$ has $T_C = 150$ K and $M_S(0) = 1.15$ μ_B/f.u. and this system no IEM was found. Instead, non-collinear structures were observed in the concentration region $0.27 \le t \le 0.65$ where B_{m1} is small.

$Y(Co_{0.88}Al_{0.12})_2$ is a very weak itinerant ferromagnet ($T_C \approx 8$ K, $M_S(0) = 0.08$ μ_B/f.u.) and shows IEM from a weak to strong ferromagnetic state at 12 T, with the magnetization increasing from $M_{Co}^{(W)} = 0.3$ μ_B/f.u. to $M_{Co}^{(S)} = 0.8$ μ_B/f.u. $Y(Co_{0.88}Al_{0.12})_2$ was hence selected to construct ferrimagnets in which transitions of different type can be realised during one magnetization process [6,35]. The magnetization curve of $(Tm_{0.25}Y_{0.75})(Co_{0.88}Al_{0.12})_2$ shown in Fig. 8 is characterized by two stepwise transitions and a region of a pronounced curvature between them. M_S for this compound is equal 0.24 μ_B/f.u. Hence, in zero field $M_{Co} = 0.84$ μ_B/f.u., i.e. this sublattice is in the strong ferromagnetic state (the molecular field

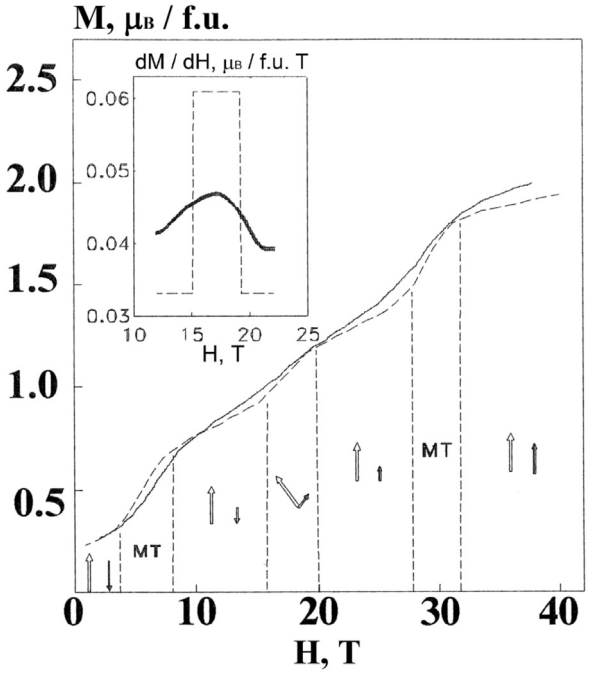

Fig. 8. The magnetization curve of $(Tm_{0.25}Y_{0.75})(Co_{0.88}Al_{0.12})_2$ [35]. The vertical dashed lines separate the different magnetic phases, the configuration of which is depicted by thick (R sublattice) and thin (Co sublattice) arrows. MT denotes the field range where IEM occurs.

$\lambda_{TmCo} M_{Tm} = 0.25$ $\mu_{Tm} \lambda_{TmCo} = 17.6$ T exceeds B_M). At low external fields, the net magnetization is $M_{Tm} - M_{Co}^{(S)}$. Since $M_{Co}^{(S)}$ is antiparallel to the external field, above the critical value $B_{m1} = \lambda_{TmCo} M_{Tm}(B_{m1}) - B_M = 6.5$ T the net magnetization becomes $M_{Tm} - M_{Co}^{(W)}$ through IEM. Between $B_{m1} = \lambda_{TmCo}(M_{Tm} - M_{Co}^{(W)}) = 15$ T and $B_{m2} = \lambda_{TmCo}(M_{Tm} + M_{Co}^{(W)}) = 19.5$ T a change from antiparallel into parallel orientation of M_{Tm} and $M_{Co}^{(W)}$ occurs through a non-collinear phase. Finally, in the parallel phase, the second metamagnetic transition occurs at $B_{m2} = \lambda_{TmCo} M_{Tm}(B_{m2}) + B_M = 29.5$ T and the net magnetization becomes $M_{Tm} + M_{Co}^{(S)}$ [35].

4. Temperature-induced IEM in RCo_3 intermetallics

In multi-sublattice R–3d intermetallics with a magnetic R and a metamagnetic d-sublattice, IEM can also be induced by temperature. Since the molecular field $B_{mol}^{(co)}$ acting on the d-subsystem decreases with increasing temperature, one can consider temperature as an additional external factor that affects the magnitude of $B_{mol}^{(Co)}$. If then the d-subsystem of such an intermetallics is in its high magnetic state at low T, the condition $B_{mol}^{(Co)}(T_m) < B_m(T_m)$ can be satisfied with increasing temperature above a certain critical value T_m, i.e., the metamagnetic sublattice will be in a low magnetic moment state above T_m. In order a temperature-induced metamagnetic transition (TIMT) to occur, the unstable sublattice is to be ferromagnetic both above and below T_m [36].

Taking into account spin fluctuations, the characteristic features of IEM can be analysed at elevated temperatures [37]. It was shown that upon reaching a critical temperature T_0, IEM becomes a transition of a second-order type and above another critical temperature T^* the upturn in the magnetization curve disappears. These conditions set a substantial restriction to the observation of TIMT: T_m shall not exceed T_0 or T^*.

TIMT has been experimentally observed in the RCo_3 series (rhombohedral $PuNi_3$-type structure) [36,38–41]. The $PuNi_3$ unit cell contains two nonequivalent crystallographic sites for *R* ions, 3*a* and 6*c*, and three sites for Co: 3*b*, 6*c*, and 18*h*. The net magnetization of the three Co sublattices in compounds with heavy *R* from Gd to Er is c.a. 1.3 μ_B/Co (see, e.g., Ref. [3]), whereas in YCo_3 M_S (= 0.6 μ_B/Co) is substantially lower. YCo_3 shows a field-induced IEM [42]. In this series, T_C changes from 300 K for YCo_3 to 612 K for $GdCo_3$, which indicates a presence of a strong intersublattice exchange interaction.

4.1. TIMT in RCo_3 compounds

Fig. 9 gives a schematic variation of M_{Co} (averaged over the three Co sites) in heavy RCo_3 compounds versus the intersublattice molecular field $B_{mol}^{(Co)}$ acting on Co at low temperatures. For $TmCo_3$ M_{Co} was evaluated using the data on the magnetovolume effect [43]. The Co sublattice is in a high magnetic state for all *R* except Tm and Y. Therefore one can expect a temperature-induced IEM in this series provided $B_{mol}^{(Co)}$ becomes equal to the critical field B_m at $T < T_0$. B_m can then be assumed to be close to the critical field of the field-induced IEM in YCo_3 ($\approx$82 T at 10 K [42]).

TIMT in the RCo_3 series has been extensively studied by thermal expansion measurements. The magnetic ordering in the itinerant electron systems is shown to be accompanied by a substantial positive volume effect $\Delta V/V > 10^{-3}$ [43], which is related with M_{Co} by a simple expression $\Delta V/V = kCM_{Co}^2$ (k being the isothermal compressibility, and C the magnetovolume coupling constant). Since the contribution of the *R* sublattice in the total $\Delta V/V$ is smaller by more than an order of magnitude, this expression can be applied for evaluating M_{Co} and determining the magnetic state of the *d*-subsystem [43].

Due to the essential scattering of the conduction electrons by spin fluctuations in the *d*-electron system, the temperature and field dependences of the electrical resistivity, $\rho(T,B)$, show remarkable anomalies near T_m. These measurements are instructive in studying TIMT in RCo_3 compounds [36].

Fig. 10 shows the temperature dependence of the volume thermal expansion of $ErCo_3$, $HoCo_3$, and $TbCo_3$. In these compounds, the molecular field acting on the Co-sublattice (the total over the 3b, 6c, and 18h sites) increases from Er to Tb. In $ErCo_3$, an abrupt change in the volume occurs at 65 K. In Ref. [38] this was accounted for a temperature-driven change in the Co magnetic state. With increasing value of $B_{mol}^{(Co)}$ the critical temperature of TIMT increases and can exceed T_0 for heavier *R*. This conclusion is in accordance with the experimental results shown in Fig. 10. In $HoCo_3$ a diffuse transition near 170 K can be seen, which is associated with the continuous change of the Co magnetic state. In $TbCo_3$ TIMT cannot be identified by thermal expansion measurements.

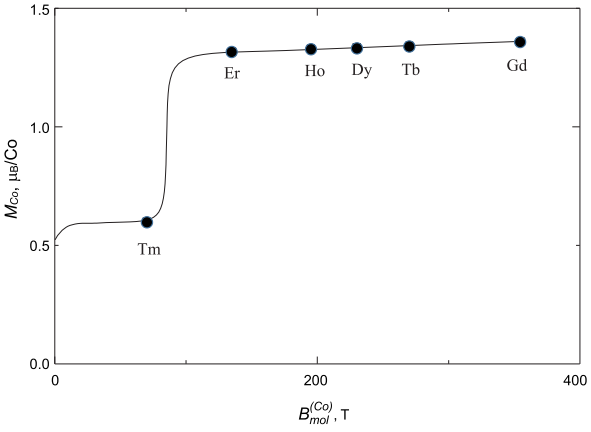

Fig. 9. A schematic variation of M_{Co} vs. $B_{mol}^{(Co)}$ in RCo_3 compounds with heavy *R*. The data were taken from Ref. [3].

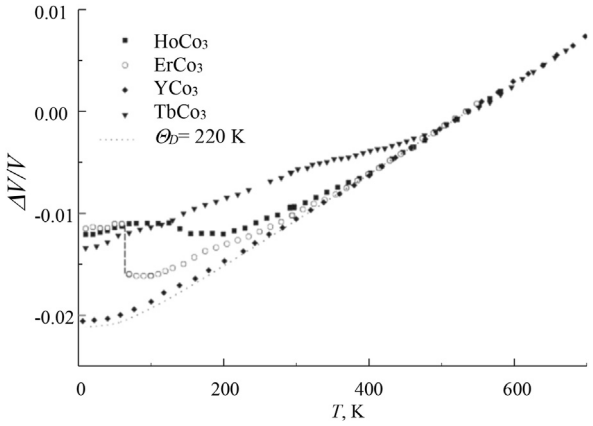

Fig. 10. Temperature dependence of the relative volume expansion of $ErCo_3$, $HoCo_3$, $TbCo_3$, and YCo_3 normalized to 550 K [38,40]. The dotted line is the Debye law plotted for Θ_D = 220 K.

Measurements of the $M(T)$ on polycrystalline $ErCo_3$ did not reveal any magnetization jump. This can be accounted for the ferrimagnetic structure of that compound. A decrease/increase in the magnetization of the Co sublattice at T_m is accompanied by a simultaneous decrease/increase in M_{Er} (since $B_{RCo}^{(Co)} \sim M_{Co}$). This circumstance strongly suppresses the resulting change of the total magnetization. A direct evidence of TIMT in RCo_3 compounds is provided by neutron diffraction data obtained from a polycrystalline sample of $ErCo_3$ (Fig. 11). The temperature dependence of the net magnetizations of both Co and Er sublattices change noticeably near T_m thus confirming the magnetic origin of the observed transitions.

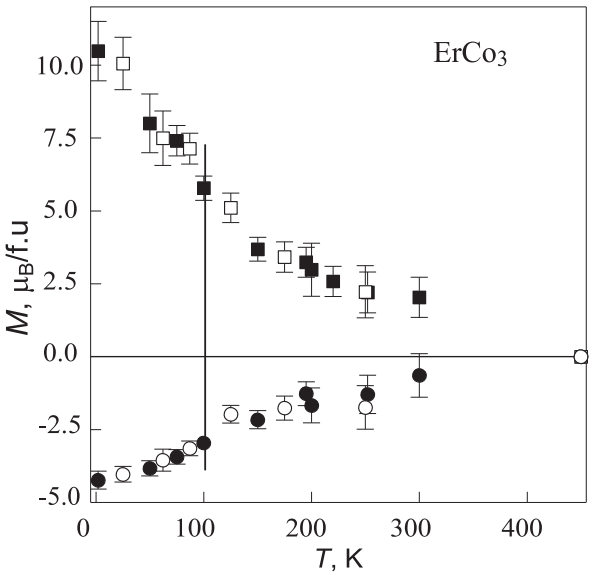

Fig. 11. Temperature variation of the magnetization of the net Er (squares) and Co (circles) sublattices in $ErCo_3$ [41]. The hollow and solid symbols correspond to measurements upon heating and cooling, respectively. The vertical dashed line shows the position of T_m.

Fig. 12 shows the $\rho(T)$ dependence of $ErCo_3$ in different magnetic fields up to 8 T. In an external field, TIMT shifts toward lower temperatures, $\partial T_m/\partial B = -0.9$ *K/T*. This tendency is a consequence of the fact that M_{Co} is oriented against the external field B_{ext} (in the case described, $M_{Co} < M_R$). Thus, the external magnetic field decreases the total effective field B_{eff} acting on the Co sublattice and TIMT occurs at lower temperatures.

4.2. Pseudobinary RCo_3 compounds

Substitution of nonmagnetic Y for magnetic *R* decreases the value of $B_{mol}^{(Co)}$. As a result a respective decrease of T_m can be expected. The thermal expansion and electrical resistivity measurements on the $Er_{1-x}Y_xCo_3$, $Ho_{1-x}Y_xCo_3$, and $Tb_{1-x}Y_xCo_3$ systems confirm this conclusion [38–40]. Based on the values of Y concentration at which $B_{mol}^{(Co)}$ becomes equal to B_m of YCo_3, the coefficients of molecular field for $ErCo_3$ and $HoCo_3$ were evaluated: $\lambda_{ErCo} = (-14.8 \pm 1.8)$ T/μ_B and $\lambda_{HoCo} = (-14.9 \pm 0.6)$ T/μ_B. They are in good agreement with the values obtained from the magnetic measurements [44]. The data available for $TbCo_3$ allowed one to estimate roughly $\lambda_{TbCo} \approx -25$ T/μ_B.

Fig. 13 shows the concentration dependence of the magnetization of the net Co sublattice of the $Er_{1-x}Y_xCo_3$ and $Ho_{1-x}Y_xCo_3$ systems at 10 K evaluated from the thermal expansion data [39–41] (*kC* was found 5×10^{-3} for both systems). The dependences obtained reflect the metamagnetic nature of the Co sublattice in these systems. The magnitude of ΔM_{Co} agrees well with that observed on the field dependence of the magnetization of YCo_3 [37].

5. R_4Co_3 series

While the two above-presented examples clearly exhibit magnetic-field or temperature induced transitions, the R_4Co_3 intermetallics do not show any phase transition although the net magnetization of the Co sublattice obviously depends on the strength of the *f-d* exchange interaction in them.

Y_4Co_3 is a very weak itinerant electron ferromagnet with $T_C \approx 5$ K and $M_S(0) \approx 0.1$ μ_B/Co. However with progressive replacement of Y by Gd the Co magnetic moment increases substantially [47]. With increasing Gd concentration in the $(Gd,Y)_4Co_3$ system, the magnetic isotherms showed a strong field dependence that was ascribed to the field dependence of the magnetization process in the Co sublattice. In Fig. 14 the Co magnetic moment, $\Delta M = M_{Gd} - M_S$, is plotted versus Gd concentration assuming the magnetic structure is collinear ferrimagnetic. As seen, a steep increase in the Co magnetization occurs for $x > 0.7$. The magnetic isotherms however do not show any evidence of phase transitions, which can be understood assuming the criteria for IEM are not fulfilled in this series.

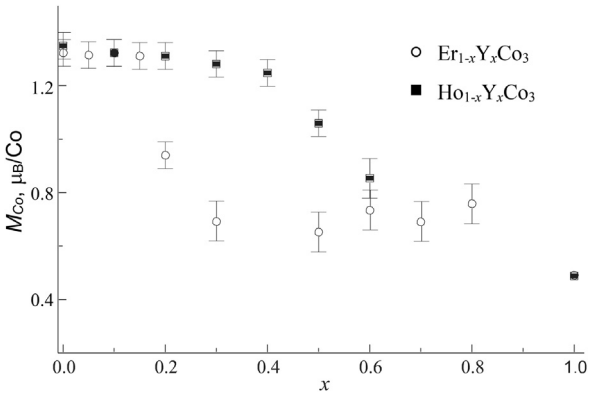

Fig. 13. Variation of the magnetic moment of the Co sublattice (averaged over the three sublattices) in the $Er_{1-x}Y_xCo_3$ and $Ho_{1-x}Y_xCo_3$ compounds versus Y concentration x at 10 K [46].

6. Conclusion

Magnetic instability in the *d*-electron subsystem (Co-sublattice) in *R*-Co intermetallics can appear not only directly as a field-induced first order magnetic phase transition. A number of other effects, such as a temperature-induced first-order magnetic phase transitions in the magnetically ordered state associated with the abrupt change of the Co magnetic moment and at the Curie point, variation of the Co magnetic moment with the strength of the *f-d* exchange interaction, decoupling of the Co and RE magnetic ordering temperatures, can be observed in these compounds due to the metamagnetic properties of the *d*-electron subsystem. Of a particular interest are the magnetization processes in ferrimagnetic *R*-Co intermetallics with one unstable magnetic sublattice, in which

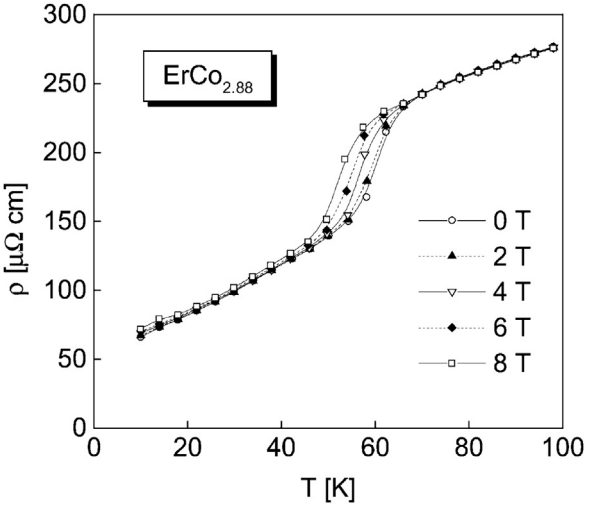

Fig. 12. Temperature dependence of the resistivity of $ErCo_3$ at different external fields [36].

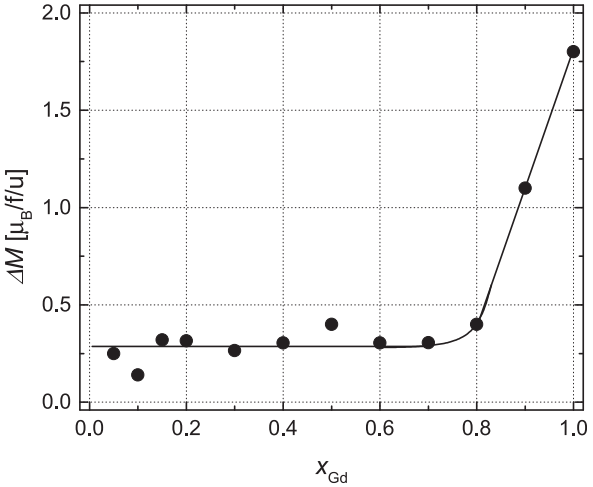

Fig. 14. The Co magnetic moment versus Gd concentration in $(Gd_xY_{1-x})_4Co_3$ intermetallic compounds (from Ref. [47]).

the contribution of Peter Brommer hardly can be underestimated. In such ferrimagnets, with careful tuning of the magnitudes of H_m, M_{Co}, M_R, and $B_{RCo}^{(Co)}$, new exotic magnetic transitions combining metamagnetism with canted magnetic structures can be observed.

References

[1] B. Barbara, D. Gignoux, C. Vettier, Lectures on Modern Magnetism, Springer-Verlag, Berlin, 1990.

[2] A.S. Markosyan, Magnetism of Alloys of 4*f* (*R*) and 3*d* Elements (*T*), Encyclopedia of Materials: Science and Technology, Elsevier Science Ltd., 2001, pp. 78–85. Vol. Magnetism.

[3] J.J.M. Franse, R. Radwanski, Magnetic properties of binary rare-earth 3*d*-transition-metal intermetallic compounds, in: K.H.J. Buschow (Ed.), Handbook on Magnetic Materials, vol. 7, Elsevier, Amsterdam, 1993, pp. 307–501. Ch. 5.

[4] N.H. Duc, T.D. Hien, P.P. Mai, N.H.K. Ngan, N.H. Sinh, P.E. Brommer, J.J.M. Franse, The magnetic phase transitions in (Tb,Ho)Co2 and (Tb,Y)Co2 compounds, Phys. B 160 (1989) 199–203.

[5] P.E. Brommer, N.H. Duc, Magnetic properties of $Tb_{1-x}Y_x(Co_{0.85}Si_{0.15})_2$ compounds, J. Magn. Magn. Mater. 262 (2003) 472–478.

[6] P.E. Brommer, I.S. Dubenko, J.J.M. Franse, F. Kayzel, N.P. Kolmakova, R.Z. Levitin, A.S. Markosyan, A.Yu. Sokolov, Field induced magnetic phase transitions in a ferrimagnet with one unstable magnetic subsystem, Phys. Lett. A 189 (1994) 253–256.

[7] P.E. Brommer, Magnetic phase diagrams for three coupled magnetic moments, Phys. B 225 (1996) 143–165.

[8] N.H. Duc, D.T. Kim Anh, P.E. Brommer, Metamagnetism, giant magnetoresistance and magnetocaloric effects in RCo_2-based compounds in the vicinity of the Curie temperature, Phys. B 319 (2002) 1–8.

[9] N.H. Duc, P.E. Brommer, Advanced magnetism and magnetic materials, in: N.H. Duc (Ed.), Aspects of Rare-earth – Transition Metal Intermetallics, vol. 1, Vietnam National University Press, 2014.

[10] N.H. Duc, P.E. Brommer, Formation of 3*d*-moments and spin fluctuations in some rare-earth intermetallic compounds, in: K.H.J. Buschow (Ed.), Handbook of Magnetic Materials, North Holland, Amsterdam, vol. 12, 1999, pp. 259–394.

[11] R.Z. Levitin, A.S. Markosyan, Itinerant metamagnetism, Sov. Phys. Uspekhi 31 (1988) 623–654.

[12] H. Yamada, T. Goto, Itinerant-electron metamagnetism and giant magnetocaloric effect, Phys. Rev. B 68 (2003) 184417.

[13] H. Yamada, Electronic structure and magnetic properties of the cubic Laves phase transition metal compounds, Phys. B 149 (1988) 390–402.

[14] J. Inoue, Electronic structure and magnetism of Y-M (M = Mn, Fe, Co and Ni) compounds, Phys. B 149 (1988) 376–389.

[15] T. Jeong, Electronic structure and magnetic properties of Y_4Co_3, Sol. State Commun. 138 (2006) 261–264.

[16] M. Shimizu, Itinerant electron metamagnetism, J. Phys. 43 (1982) 155–163.

[17] T. Goto, T. Sakakibara, K. Murata, H. Komatsu, K. Fukamichi, Itinerant electron metamagnetism in YCo_2 and $LuCo_2$, J. Magn. Magn. Mater. 90&91 (1990) 700–702.

[18] V.V. Aleksandryan, A.S. Lagutin, R.Z. Levitin, A.S. Markosyan, V.V. Snegirev, Metamagnetism of the itinerant *d*-electrons in YCo_2: investigation of the metamagnetic transitions in $Y(Co_{1-x}Al_x)_2$, Zh. Eksp. Teor. Fiz. 89 (1985) 271–276.

[19] T. Sakakibara, T. Goto, K. Yoshimura, M. Shiga, Y. Nakamura, Itinerant electron metamagnetism in $Y(Co_{1-x}Al_x)_2$, Phys. Lett. A 117 (5) (1986) 243246.

[20] I.L. Gabelko, R.Z. Levitin, A.S. Markosyan, V.I. Silant'ev, V.V. Snegirev, Influence of the d-electron concentration on the itinerant electron metamagnetism and ferromagnetism in $M(Co_{1-x}Al_x)_2$ systems (M = Y, Lu): study of compounds with non-variable crystal cell parameter, J. Magn. Magn. Mater. 94 (1991) 287–292.

[21] T. Goto, H.A. Katori, T. Sakakibara, H. Mitamura, K. Fukamichi, K. Murata, Itinerant electron metamagnetism and related phenomena in Co-based intermetallic compounds, J. Appl. Phys. 76 (1994) 6682–6687.

[22] M. Aoki, H. Yamada, Electronic structure and magnetism of *C*15-type Laves phase compounds $Y(Co,Al)_2$ and $Y(Co,Si)_2$, Phys. B 177 (1992) 259–261.

[23] E. Gratz, A.S. Markosyan, Physical properties of RCo_2 Laves phases, J. Phys. Condens. Matter 13 (2001) R385–R413.

[24] E. Gratz, R. Hauser, A. Lindbaum, M. Maikis, R. Resel, G. Schaudy, R.Z. Levitin, A.S. Markosyan, I.S. Dubenko, A.Yu. Sokolov, S.W. Zochowski, Gd substitutions in the $TmCo_2$ Laves phase: the onset of long-range magnetic order in the itinerant subsystem, J. Phys. Condens. Matter 7 (1995) 597–610.

[25] P.E. Brommer, I.S. Dubenko, J.J. Franse, R.Z. Levitin, A.S. Markosyan, R.J. Radwański, V.V. Snegirev, A.V. Sokolov, Field-induced non-collinear magnetic structures in Al-stabilized RCo_2 Laves phases. Study of the $Lu_{1-y}Tm_y(Co_{0.88}Al_{0.12})_2$ system, Phys. B 183 (1993) 363–368.

[26] R.Z. Levitin, A.S. Markosyan, V.V. Snegirev, Band metamagnetism in the Co sublattice in $Er_{1-x}Y_xCo_2$, Phys. Met. Metallogr. 57 (1984) 274–283.

[27] H. Wada, M. Shiga, H.A. Katori, M.I. Bartashevich, T. Goto, Anomalous magnetization process of $Er_{1-x}Lu_xCo_2$, Phys. B 201 (1994) 139–142.

[28] R. Hauser, C. Kussbach, R. Grössinger, G. Hilscher, Z. Arnold, J. Kamarad, A.S. Markosyan, E. Chappel, G. Chouteau, On the metamagnetic state in $Er_{1-x}T_xCo_2$, (T = Y, Tm) compounds, Phys. B 294–295 (2001) 182–185.

[29] N.H. Duc, T. Goto, Itinerant electron metamagnetism of Co sublattice in the lanthanide-cobalt intermetallics, in: K.A. Gschneidner Jr., L. Eyring (Eds.), Handbook on the Physics and Chemistry of Rare Earths, vol. 26, Elsevier, Amsterdam, 1999, pp. 177–264. Ch. 171.

[30] D. Bloch, D.M. Edwards, M. Shimizu, J. Voiron, 1st order transitions in ACo_2 compounds, J. Phys. 5 (1975) 1217–1226.

[31] R. Hauser, E. Bauer, E. Gratz, H. Müller, M. Rotter, H. Michor, G. Hilscher, A.S. Markosyan, K. Kamishima, T. Goto, Decoupling of the magnetic ordering of the rare earth and the Co sublattices in $Er_{1-x}Y_xCo_2$ compounds driven by substitution or pressure, Phys. Rev. B 61 (2000) 1198–1210.

[32] S.V. Tyablikov, Methods of Quantum Theory of Magnetism, Nauka, Moscow, 1965.

[33] I.S. Dubenko, N.P. Kolmakova, R.Z. Levitin, A.S. Markosyan, A.K. Zvezdin, Magnetic phase diagrams and magnetization curves of ferrimagnets with one unstable magnetic subsystem, J. Magn. Magn. Mater. 153 (1996) 207–214.

[34] M. Bartashevich, T. Goto, I.S. Dubenko, N.P. Kolmakova, S.A. Kolongii, R.Z. Levitin, A.S. Markosyan, Two-step-like magnetization curves of $YR(CoAl)_2$, R = Ho, Er, in fields up to 100 T, Phys. B 246–247 (1998) 487–490.

[35] P.E. Brommer, I.S. Dubenko, J.J.M. Franse, F. Kayzel, N.P. Kolmakova, R.Z. Levitin, A.S. Markosyan, A. Yu Sokolov, Phase transitions induced by magnetic field in ferrimagnets with one unstable magnetic subsystem, Phys. B 211 (1995) 155–157.

[36] E. Gratz, A.S. Markosyan, I.Yu. Gaidukova, V.E. Rodimin, St Berger, E. Bauer, H. Michor, Temperature induced itinerant electron metamagnetism in $ErCo_3$ and $HoCo_3$: influence of an external field and pressure, Sol. State Commun. 120 (2001) 191–194.

[37] T. Goto, K. Fukamichi, H. Yamada, Itinerant electron metamagnetism and peculiar magnetic properties observed in 3*d* and 5*f* intermetallics, Phys. B 300 (2001) 167–185.

[38] N. Ali, I.S. Dubenko, I.Yu. Gaidukova, A.S. Markosyan, V.E. Rodimin, Temperature induced magnetic instability in the itinerant Co subsystem of the $Er_{1-x}Y_xCo_3$ compounds, Phys. B 281–282 (2000) 696–698.

[39] I.S. Dubenko, I.Yu Gaidukova, E. Gratz, K. Inoue, A.S. Markosyan, V.E. Rodimin, Magnetic instability of the Co sublattice in the $Ho_{1-x}Y_xCo_3$ system, Phys. B 319 (2002) 21–27.

[40] I.Yu Gaidukova, A.S. Markosyan, V.E. Rodimin, Temperature-induced itinerant metamagnetism in $R_{1-x}Y_xCo_3$ systems (R = Ho, Tb), J. Magn. Magn. Mater. 258–259 (2003) 574–576.

[41] E. Gratz, A.S. Markosyan, V. Paul-Boncour, A. Hoser, N. Stuesser, I.Yu. Gaidukova, V. Rodimin, Temperature induced itinerant electron metamagnetism in $ErCo_3$ studied by neutron diffraction, Appl. Phys. A 74 (2002) S698–S700.

[42] T. Goto, H.A. Aruga Katori, T. Sakakibara, M. Yamaguchi, Co anisotropy in YCo_3, Phys. B 177 (1992) 255–258.

[43] A.V. Andreev, Thermal expansion anomalies and spontaneous magnetostriction in *R-T* intermetallics (*T*=Co and Fe), in: K.H.J. Buschow (Ed.), Handbook of Magnetic Materials, vol. 8, North-Holland, Amsterdam, 1995, pp. 59–187.

[44] T. Goto, M.I. Bartashevich, H. Aruga Katori, Ye.V. Shcherbakova, A.S. Yermolenko, Field-induced transitions of RCo_3 (R = Ho, Er and Tm) in ultrahigh magnetic fields up to 110 T, Phys. B 211 (1995) 131–133.

[45] I.S. Dubenko, I.V. Golosovsky, E. Gratz, R.Z. Levitin, A.S. Markosyan, I. Mirebeau, S.V. Sharygin, Neutron diffraction study of magnetic properties of $TmCo_2$, J. Magn. Magn. Mater. 150 (1995) 304–310.

[46] A.S. Markosyan, V.E. Rodimin, Temperature-induced itinerant electron metamagnetism, J. Magn. Magn. Mater. 300 (2006) e518–e521.

[47] E. Gratz, V. Sechovsky, E.P. Wohlfarth, H.R. Kirchmayr, The magnetic and transport properties of the compounds $(Gd,Y)_4Co_3$, J. Phys. F. Metal. Phys. 10 (1980) 2819–2829.